Cirrus Horizontal Heterogeneity and 3-D Radiative Effects on Cloud Optical Property Retrievals From MODIS Near to Thermal Infrared Channels as a Function of Spatial Resolution

T. Fauchez, S. Platnick, O. Sourdeval, C. Wang, K. Meyer, C. Cornet, F. Szczap

HAL Id: insu-03686251
https://insu.hal.science/insu-03686251

Submitted on 3 Jun 2022

Check for updates

RESEARCH ARTICLE

Key Points:
- Below ~1-km horizontal spatial resolution, NIR/SWIR reflectance-based retrievals have the largest retrieval errors due to 3-D radiative effect
- Above ~1-km spatial resolution, TIR radiance-based retrievals have the largest retrieval errors due to cloud horizontal heterogeneity
- Cloud optical retrievals from multispectral measurements can be severely impacted by the wavelength dependency of cloud heterogeneities and 3-D radiative effects

Correspondence to:
T. Fauchez,
thomas.j.fauchez@nasa.gov

Cirrus Horizontal Heterogeneity and 3-D Radiative Effects on Cloud Optical Property Retrievals From MODIS Near to Thermal Infrared Channels as a Function of Spatial Resolution

T. Fauchez[1,2] (ID)**, S. Platnick[2]** (ID)**, O. Sourdeval[3], C. Wang[2,4]** (ID)**, K. Meyer[2], C. Cornet[5], and F. Szczap[6]**

[1]Universities Space Research Association, Columbia, MD, USA, [2]NASA Goddard Space Flight Center, Greenbelt, MD, USA, [3]Institute for Meteorology, Faculty of Physics and Earth Sciences, University of Leipzig, Leipzig, Germany, [4]Earth System Science Interdisciplinary Center, University of Maryland, College Park, MD, USA, [5]Laboratoire d'Optique Atmosphérique, UMR 8518, Université Lille 1, Villeneuve d'Ascq, France, [6]Laboratoire de Météorologie Physique, UMR 6016, Université Blaise Pascal, Clermont Ferrand, France

Abstract To retrieve cloud optical properties, current satellite operational imager algorithms simplify the forward radiative transfer problem by assuming that cloudy pixels are horizontally homogeneous and radiatively independent. This study investigates the effects of cirrus horizontal heterogeneity and 3-D radiative effects on cloud optical thickness (COT) and ice crystal effective radius (CER) retrievals obtained using simulated nadir near-infrared/shortwave-infrared (NIR/SWIR) reflectances at 0.86 and 2.13 μm and thermal infrared (TIR) radiances at 8.5, 11.0, and 12.0 μm, first separately and next using the five wavelengths together. Synthetic cirrus radiation fields are generated using a cirrus 3-D cloud generator and a 3-D radiative transfer code. When both cloud 3-D and heterogeneity effects are considered, the solar reflectance-based retrievals have the largest errors (up to 10% for COT and 80% for CER, depending on solar angles) for spatial resolutions less than 500–1,000 m, while the TIR-based retrievals have the largest errors (up to 30% for COT and 50% for CER) above this resolution due to parallel homogeneous approximation bias. Therefore, TIR radiance-based retrievals are preferable for spatial resolutions equal or higher than ~500 m to 1 km, while NIR/SWIR reflectance-based retrievals are preferable for coarser spatial resolutions. The combination of NIR/SWIR and TIR measurements performed better together than individually for CER retrieval only for resolutions coarser than 2.5 km because 3-D effects are negligible at this scale. Thus, the spectral dependence of subpixel cloud horizontal heterogeneity and 3-D radiative effects has strong consequences when simultaneously using different channels for retrieving cirrus properties.

1. Introduction

Clouds are one of the major uncertainties in climate prediction (IPCC AR5 report; Boucher et al., 2013). Ice clouds such as cirrus are located in the high troposphere and have a large temporal and spatial coverage leading to a significant impact on Earth's radiative budget (Lynch et al., 2002; Matus & L'Ecuyer, 2017; Oreopoulos et al., 2017). Cirrus clouds are composed of ice crystals with very complex shapes (habits) leading to wide ranges in microphysical and optical properties, as well and macrophysical heterogeneity. This complexity makes it challenging to quantify the cirrus radiative effect (Baran, 2009). Ice clouds may therefore lead to significant uncertainties in climate simulations if their properties are not properly constrained (Baran, 2009; Fusina et al., 2007; Sanderson et al., 2008; Zhang et al., 1999, and references therein). It is therefore crucial to precisely understand and quantify the uncertainties on the retrieval of ice cloud properties in order to evaluate and further improve model realizations and thereby climate prediction.

Imager measurements allow for a limited number of cloud parameter retrievals because (i) the number of available spectral channels is limited and (ii) the information content is limited. Global passive satellite retrievals infer cirrus properties from solar reflectance (e.g., Platnick et al., 2017 for the Moderate Resolution Imaging Spectroradiometer [MODIS]) and/or thermal radiance measurements (e.g., Garnier et al., 2012, 2013 for the Imaging Infrared Radiometer). MODIS retrieval methods use a combination of visible (VIS: 0.4–0.7 μm) and near-infrared (NIR: 0.75–0.95 μm), short-wave infrared (SWIR: 0.9–1.7 μm), and midwave-infrared (3–5 μm) spectral channels (e.g., MODIS Collection 6; Platnick et al., 2017) as well as thermal-

infrared (TIR: 8–15 μm) channels (e.g., CERES-MODIS products; Minnis et al., 2011). Thermal infrared retrieval techniques use for the Advanced Very High Resolution Radiometer (Parol et al., 1991) and IIR onboard CALIPSO (Garnier et al., 2012, 2013) are based on the split-window technique (Inoue, 1985; Parol et al., 1991). This technique retrieves cloud optical thickness (COT) and crystal effective radius (CER) from the brightness temperature (BT) difference of two different channels in the infrared atmospheric windows where gaseous absorption is small. Based also on TIR spectral information, an optimal estimation method (OE; Rodgers, 2000) is used for the Atmospheric Infrared Sounder V6 (AIRS; Kahn et al., 2014, Kahn et al., 2015). Other imager products, including the Pathfinder Atmospheres-Extended (PATMOS-x) Advanced Very High Resolution Radiometer product (Heidinger et al., 2014), use a combination of solar reflectances and thermal infrared radiances to estimate cloud optical properties and cloud-top temperature, respectively. Further, the research-level codes of Cooper et al. (2007), Wang, Platnick, Zhang, Meyer, Yang (2016), and Wang, Platnick, Zhang, Meyer, Wing et al. (2016) for MODIS and of Sourdeval et al. (2015, 2016) for several A-train instruments take advantage of solar reflectance and terrestrial TIR radiance information content. Comparing the solar and thermal method, Cooper and Garrett (2010) showed, using MODIS data, that a space-based infrared split-window technique is more suitable for cirrus retrievals than a visible near-infrared (VNIR)-SWIR technique, as long as the cirrus is optically thin enough, that is with a visible optical thickness between roughly 0.5 and 3 and with CER smaller than 20 μm; this is because cirrus clouds emit at a much colder temperature than the surface leading to a larger contrast with clear-sky radiances than the cirrus/surface contrast in solar reflectance channels. In addition, it has been shown that VNIR/SWIR retrieval techniques have higher uncertainties in high-latitude regions and optically thin cirrus cloud scenes (Wang, Platnick, Zhang, Meyer, Yang, 2016). Furthermore, TIR retrieval algorithms can be applied to both daytime and nighttime conditions, a distinct benefit compared to solar-reflectance methods for developing ice cloud climatologies.

However, regardless of the operational retrieval method, the lack of information regarding the 3-dimensional (3-D) cloud structure and computing time limitations impose the simplified assumption of a flat and homogeneous cloud at the pixel-level scale, that is, the so-called plane-parallel homogeneous approximation (PPH; Cahalan et al., 1994). In addition, a cloudy pixel is considered to be radiatively independent of its neighboring pixels (no horizontal transport of radiation), which is the independent pixel approximation (Cahalan et al., 1994) or independent column approximation (Stephens et al., 1991). Such representation assumes that the radiative transfer (RT) is one-dimensional in the vertical dimension that considerably reduces the RT calculation time; note that while some techniques have been developed to reduce 3-D RT computation time in the TIR (Fauchez, Davis et al., 2017), they are currently not sufficiently mature to be implemented operationally.

Many studies have been conducted in the solar spectral range to better understand the impact of cloud heterogeneities on cloud optical property retrievals, primarily on warm clouds such as stratocumulus (Kato & Marshak, 2009; Varnai & Marshak, 2001; Zhang et al., 2012; Zhang et al., 2016; Zhang & Platnick, 2011; Zinner et al., 2010; Zinner & Mayer, 2006).Those studies have shown that the sign and amplitude of retrieval errors (tens of percent) on cloud optical properties and/or cloud albedo depend on numerous factors, such as the spatial resolution, wavelength, geometry of observation, and cloud morphology.

Studies on the effects of cirrus cloud heterogeneities on TIR retrievals include Fauchez et al. (2012, 2014), who showed that neglecting cloud horizontal heterogeneity for a 1-km spatial resolution radiometer may lead to a TOA BT bias up to 15 K. Concerning retrieved cloud properties, Fauchez et al. (2015) showed, by modeling a cirrus cloud observed during the CIRCLE 2 airborne campaign (Sourdeval et al., 2012), that cirrus horizontal and vertical heterogeneities in the TIR result in an overestimation of retrieved CER by 13% and 20%, respectively, and an underestimation of the retrieved COT by 5% and 7%, respectively. Biases can be even larger for thicker cirrus and smaller ice crystals, up to 50% and 100% for COT and CER, respectively. Zhou et al. (2017) found similar results for solar reflectance retrievals with COT underestimated by 1 to 24% and CER overestimated by 0.6–15 μm, depending on cirrus characteristics, sensor settings, and solar zenith angles. Fauchez, Platnick, Meyer et al. (2017) and Fauchez et al. (2018) studied the impact of horizontal heterogeneity and 3-D effects on the TOA radiation in the TIR and NIR/SWIR, from 50-m to 10-km spatial resolution. The effects are at a minimum between 100- and 250-m spatial resolution in the TIR, but NIR/SWIR solar geometries make estimating the scale of minimum effects difficult to determine.

These previous works concern either solar radiation or thermal radiation, but none of them shows how the spectral and spatial dependence of cloud heterogeneities and 3-D radiative effects impacts the cirrus

optical property retrievals. This is the point of this paper. In section 2 we will present the method used in this study. In section 4 we will discuss the retrieval of cirrus optical properties with an OE using either TIR channels, NIR/SWIR channels, or a combination of TIR, NIR, and SWIR as a function of the spatial resolution. Comparisons of the simulated retrieval errors with MODIS data and the estimation of retrieval errors due to cirrus heterogeneity and 3-D effects for various space-borne radiometer resolutions are presented in section 5. Conclusions and perspectives will be highlighted in section 5.

2. Materials and Methods

2.1. Cloud Simulation

Cirrus clouds, which include related subtypes cirrostratus and cirrocumulus (American Meteorological Society, 2012; Heymsfield et al., 2017), have a variety of macroscale and visual (i.e., heterogeneity and texture) properties at different averaging scales. Kuo et al. (1988), using Landsat imagery, showed the fractal nature of cirrus. Invariant scale properties of cirrus (i.e., properties of fractal object) are rather studied by the analysis of the "so-called" β spectral slope (i.e., the slope of the logarithm of the energy of the analyzed signal as the function of the logarithm of wave number; Hogan & Kew, 2005; Szczap et al., 2014). The heterogeneity of the cloud is often characterized by the ρ inhomogeneous parameter (Davis et al., 1997; Szczap et al., 2000) or the fractional standard deviation (FSD), both defined as the standard deviation divided by the mean (Shonk et al., 2010). Fauchez, Platnick, Meyer et al. (2017) present a short review about heterogeneity of macroscale and optical properties of cirrus and summarize the range and mean values from scientific literature (0.1 to 1.5 for the value of the inhomogeneous parameter) that we used in this study. These mean values are also corroborated by the work of Alkasem et al. (2017). From CloudSat satellite data, Hill et al. (2012, 2015) developed a parameterization of ice cloud FSD suitable for inclusion in general circulation models. They found that FSD is a complex function of the cloud cover and increases with horizontal scale and with the thickness of the layer and furthermore is a function of cloud regime wherein greater values of FSD are observed in convective clouds. From Atmospheric Radiation Measurement ground-based observations, Ahlgrimm and Forbes (2016) confirm that the FSD of isolated cirrus clouds, at 80-km scale, falls largely within the range of parameterized values from Hill et al. (2015). Ahlgrimm and Forbes (2017) refined the formulation by Hill et al. (2015), wherein FSD is dependent on total water and is enhanced for convective situations based on the detrainment ratio.

The cirrus cloud structure used in this study is generated by the 3DCLOUD model (Szczap et al., 2014) used in Fauchez, Platnick, Sourdeval et al. (2017), Fauchez, Platnick, Meyer et al. (2017), and Fauchez et al. (2018). It consists of a fallstreak structure with a mean COT of 1.4 at 12.03 μm wavelength, an inhomogeneous parameter $\rho_{COT} = \left[\sigma_{COT}/\overline{COT}\right] = 1.0$, and cloud top and base altitudes at 10 and 12 km, respectively. The optical thicknesses at 12.03 μm for this cirrus ranges from 0.008 to about 12.

Cirrus optical properties are parameterized using the same microphysical model assumed by the MODIS Collection 6 cloud product, namely, the severely roughened single-habit column aggregate from Yang et al. (2013). The cloud is assumed to have a constant CER of 10 μm. The atmosphere is set to a standard midlatitude summer. The use of a CER of 10 μm is mainly constrained by the TIR retrieval, since TIR techniques are often limited to CER up to 20 μm (Dubuisson et al., 2008; Garnier et al., 2012; Parol et al., 1991). Thus, in order to look at the impact of cloud horizontal heterogeneity and 3-D radiative effects on CER retrievals, we must select a CER for which the retrieval technique is sensitive.

2.2. Radiative Transfer Simulations

Radiative transfer simulations have been performed with the 3DMCPOL (Cornet et al., 2010; Fauchez et al., 2014) model. This code uses a forward Monte Carlo method to compute radiances or reflectances from MODIS NIR to the TIR channels following either a 3-D RT or a 1-D RT approximation. Cyclic boundary conditions are imposed at the edges of the domain. For NIR/SWIR reflectances and TIR radiances (BTs), one hundred billion fictive light particles (Pujol, 2015; referenced hereafter as photons) per 3-D computation of solar reflectances at 50-m spatial resolution are computed with 3DMCPOL in 3.5 core days (resp. 10 core days) on 2,048 parallel cores of the NCCS discover supercomputer (see acknowledgements). 1-D simulations are more computationally expensive because they have to be computed at each spatial resolution ranging from 50 m to 10 km (for a total of 52,121 simulated pixels). Roughly 1 and 2 months are needed for one NIR/SWIR reflectance channel and one TIR radiance channel, respectively, to compute the simulations for every spatial
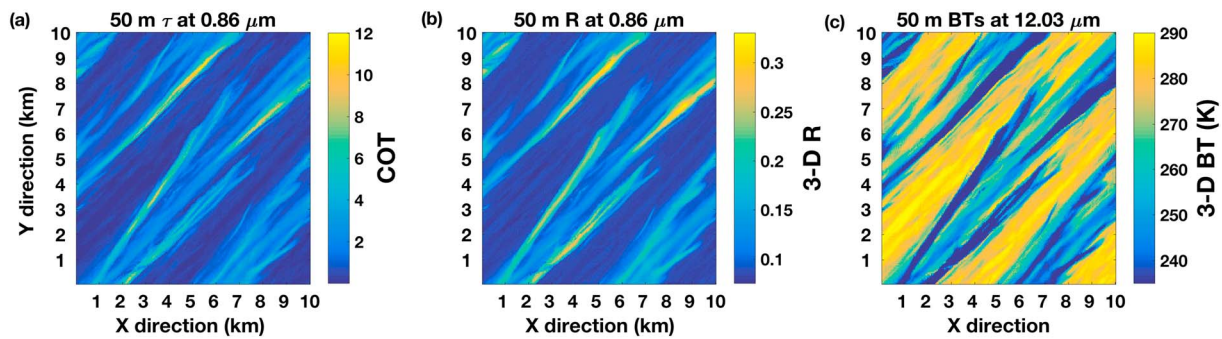
Figure 1. (a) Optical thickness field, (b) 0.86-μm reflectance field, and (c) 12.03-μm brightness temperature field at 50-m spatial resolution.

resolution and for all solar angles (solar reflectances only). The reflectance accuracy is about 0.1%, and the BT accuracy is about 0.4 K. Note that the reflectance accuracy is far below the MODIS reflectance uncertainty of 3% reported by Xiong et al. (2005, 2017).

Figure 1 shows the cirrus optical thickness field (a) and its corresponding 0.86-μm reflectance (b) and 12.03-μm radiance (c) 3-D fields.

2.3. Cloud Optical Property Retrievals

To retrieve cirrus cloud optical properties with multichannel information from simulated MODIS observations, we use the multilayer (ML) research-level OE method (Rodgers, 2000) developed by Sourdeval et al. (2015, 2016). This method merges the information contained in five radiometric channels ranging from the visible to the thermal infrared to simultaneously retrieve ice and liquid cloud properties.

The OE method is based on the estimation of the cost function, expressed in equation (1), that provides a quantitative estimate of the consistency of the retrievals with respect to the measurements and a priori assumptions. The first term on the right-hand side of equation (1) expresses the consistency between the measurements **y** and the forward model simulations F obtained from the retrieved state **x**. In other words, a very small cost function (i.e., smaller than the number of measurements; Marks & Rodgers, 1993) indicates that the retrieved properties allow the forward model to fit the measurements at all wavelengths. This consistency is weighted by instrumental errors and by uncertainties on fixed (i.e., nonretrieved) parameters used in the forward model, such as atmospheric profiles of temperature and gas concentrations or the surface albedo and temperature. A list and values of these uncertainties can be found in Sourdeval et al. (2015). In this study, the instrumental errors are set to 3% for the shortwave reflectances (Xiong et al., 2005, 2017) and 0.5 K for the TIR BTs. The second term on the right-hand side of equation (1) quantifies the agreement between the retrieved state and its a priori value, weighted by the errors assumed on the latter. This therefore provides information on the reduction of the a priori state space by the measurements. Typically, this state is chosen to be large enough so that a priori assumptions do not overly constrain the retrievals. In this study, a Gaussian distribution with a mean of 7 μm and a standard deviation of 10 μm are considered for CER, and a log-normal distribution with a geometric mean of 0.7 and a geometric standard deviation of 1.0 are selected for COT. These should encompass a wide range of realistic COT and CER values encountered in cirrus clouds. Sensitivity analysis and comparisons (not shown here) with another OE method (Wang, Platnick, Zhang, Meyer, Yang, 2016; Wang, Platnick, Zhang, Meyer, Wing et al., 2016) have been performed to verify that the following results do not largely depend on choices made on a priori estimates, in particular by repeating the analyses for different a priori CER.

$$\varnothing = [\boldsymbol{y} - F(\boldsymbol{x})]^T \boldsymbol{S}_{\in}^{-1}[\boldsymbol{y} - F(\boldsymbol{x})] + [\boldsymbol{x} - \boldsymbol{x_a}]^T \boldsymbol{S}_a^{-1}[\boldsymbol{x} - \boldsymbol{x_a}] \tag{1}$$

Multilayer theoretical capabilities have thoroughly been investigated in a wide range of atmospheric conditions (Sourdeval et al., 2015), and its global retrievals have been evaluated against numerous active and passive A-Train operational products (Sourdeval et al., 2016). It was concluded that this OE is capable of retrieving the properties of ice clouds ranging from optically thin (COT ~0.05) to very thick (COT ~40) clouds due to the combination of visible and thermal infrared measurements. This retrieval code has already been used in

Fauchez, Platnick, Sourdeval et al. (2017) to retrieve cloud optical properties at the 1-km MODIS observation scale using either TIR, or NIR and SWIR, or a combination of five channels across the TIR, NIR, and SWIR. They found that when the three wavelength regions are combined, heterogeneity effects are dominated by the NIR horizontal radiative transport effect leading to overestimated small COTs (by a few percent) and underestimated large COTs (by tens of percent). However, retrieved effective diameters from NIR/SWIR measurements were found to be weakly affected (few percent) by heterogeneity and 3-D effects, contrary to retrievals using TIR channels only showing a larger impact (up to 100%).

2.4. Cirrus Horizontal Heterogeneity and 3-D Effects

Horizontal heterogeneity effects leading to the plane-parallel and homogeneous (PPH) bias are due to the nonlinearity between optical properties and radiance/reflectance. The horizontal heterogeneity depends on the optical thickness variability inside the observation pixel, often represented by the standard deviation (Fauchez et al., 2014) or the inhomogeneous parameter (i.e., the standard deviation normalized by the mean value; Szczap et al., 2014). In addition, 3-D effects are due to the horizontal transport of radiation across multiple pixels.

Both effects are strongly dependent on the sensor spatial resolution. The subpixel heterogeneity effects tend to increase with coarser spatial resolutions, while 3-D effects due to nonindependent pixels increase with finer spatial resolutions and impacts of both are dependent on the wavelength. In addition, at solar wavelengths, illumination and shadowing effects for solar zenith angles off nadir will introduce additional biases into the cloud optical properties retrievals. Therefore, for retrieval techniques such as OE that use multiple channels across the NIR, SWIR, and TIR spectrum, spectral differences in horizontal heterogeneity and 3-D effects can potentially lead to retrieval biases and/or a degradation of the retrieval uncertainty. In the next section, we will present the impact of horizontal heterogeneity and 3-D effects from 50-m to 10-km spatial resolutions using either NIR/SWIR channels, TIR channels, or a combination of NIR/SWIR and TIR channels.

3. Multiwavelength, Multispatial Resolution Retrievals of Cirrus Optical Properties

3.1. Horizontal Heterogeneity Effect

In this section, only the horizontal heterogeneity effects on the COT (Δ**COT**) and effective radius (Δ**CER**) retrievals are considered. These two quantities are estimated using the following steps:

1. High spatial resolution (50 m) TIR radiances and/or NIR/SWIR reflectances from 1-D RT calculations are averaged to spatial resolutions from 100 m to 10 km.
2. Retrieved optical properties are obtained from the averaged 1-D radiances/reflectances.
3. True optical properties are estimated from 50-m optical properties (**COT** only is averaged because **CER** is set to 10 **μm** for entire cloud layer), linearly averaged to a spatial resolution from 50 m to 10 km.
4. True optical properties are subtracted from retrieved optical properties to obtain Δ**COT** and Δ**CER**.

Figure 2 shows $-\Delta$**COT** and Δ**CER** (estimated from 1-D RT only) as a function of the spatial resolution using TIR channels (8.53, 11.01, and 12.03 **μm**) only (blue lines), NIR/SWIR channels (0.86 and 2.13 **μm**) only (red lines), and the combination of the five channels across the three wavelength ranges (black lines). For the last two retrievals, five solar zenith angles are considered. We plot $-\Delta$**COT** instead of Δ**COT** to keep a positive difference like Δ**CER**. As expected, for the TIR and TIR + NIR/SWIR channel combinations,$-\Delta$**COT** increases when downgrading spatial resolution because of the large PPH bias in the TIR. Indeed, for this COT range, the TIR BTs have the largest curvature (nonlinear effect) that maximizes the PPH bias, while the VNIR/SWIR radiances have a weak nonlinear effect. We can also see that $-\Delta$**COT** is minimized when retrieved from NIR/SWIR measurements, followed by the TIR + NIR/SWIR (but with a larger cost function), and finally, TIR only Δ**CER** is the greatest above 500 m for the TIR, again because of the larger PPH bias. Note that TIR and NIR/SWIR cost functions are very close to each other and are almost indiscernible on the figure. Their very small cost function values of about 1 (right column) remain low and constant for all spatial resolutions, which indicates that the retrieved **COT** and CER provide an accurate reproduction of the simulated measurements.Overall, considering only 1-D RT computations, $-\Delta$**COT** and Δ**CER** changes with respect to the solar zenith angles Θ_s or azimuth angle Φ_s are small. When Θ_s increases, $-\Delta$**COT** for NIR/SWIR and (TIR + NIR/SWIR) slightly increases especially for large spatial resolutions because of the
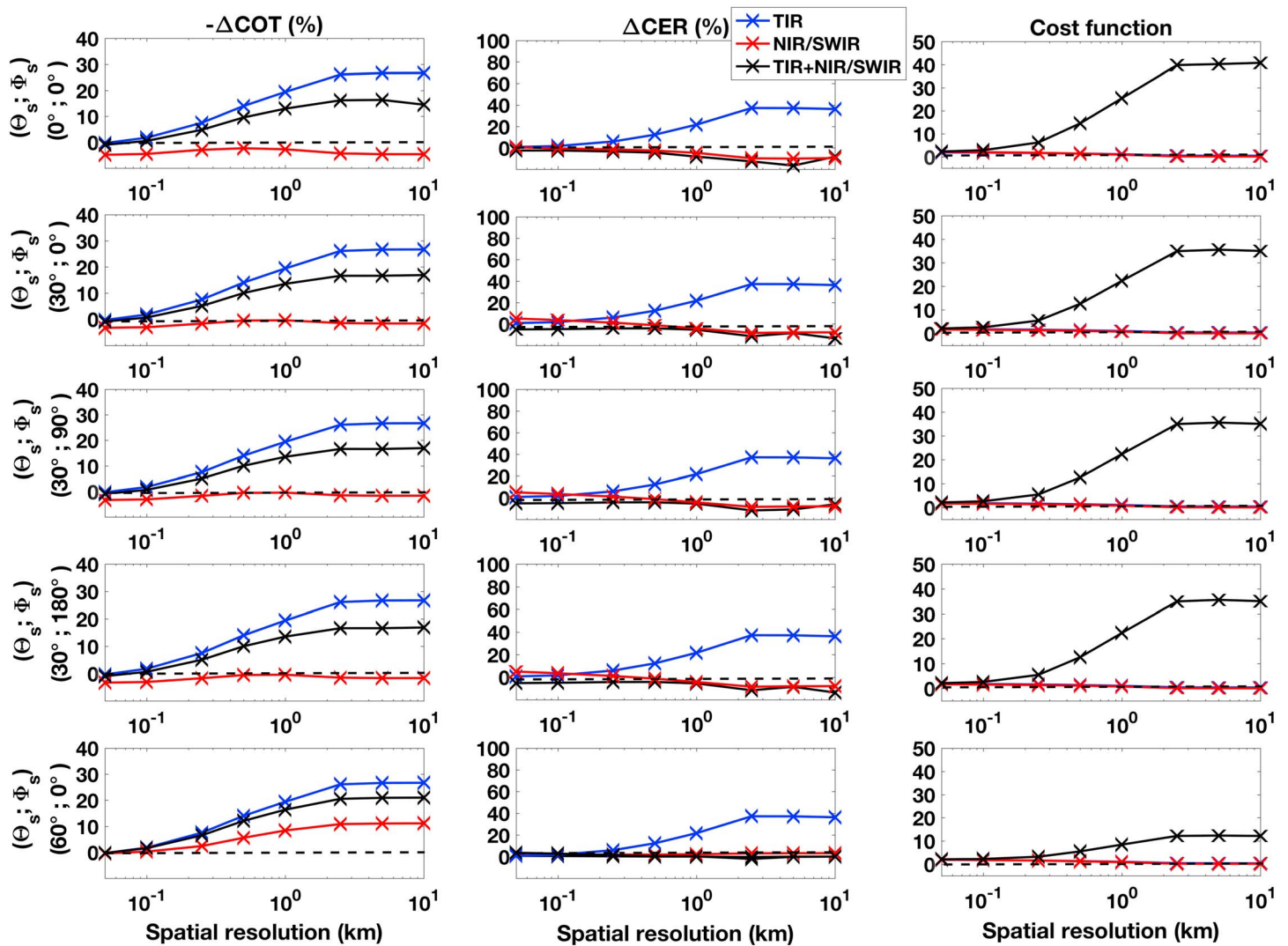
Figure 2. Errors on the (left column) optical thickness and (middle column) effective radius due to cloud horizontal heterogeneity only (RT computation are 1-D) and the (right column) associated cost function retrieved with an OE in the TIR, NIR/SWIR, and TIR + NIR/SWIR ranges as a function of the spatial resolution and for various solar zenith (θ_s) and azimuth (ϕ_s) angles. Note that the TIR and NIR/SWIR cost functions appear very close to each other.

dependence of the PPH bias with solar geometries (Fauchez et al., 2018), getting closer to the TIR values while ΔCER is slightly reduced at $\Theta_s = 60^{\circ}$. Interestingly, the combination of the five channels shows the smallest ΔCER (~0% to −10%), which is almost independent of the spatial resolution. Note that the negative ΔCER is associated with a high cost function (~40) illustrating the difficulty that the OE has to converge on a single solution from NIR/SWIR reflectances and TIR radiances. Below 500 m, horizontal heterogeneity effects are negligible for both the TIR and NIR/SWIR ranges (Fauchez, Platnick, Meyer et al., 2017); thus, retrievals from both are close to the real mean optical property from a 1-D homogenous field leading to a small cost function. For RT computations at 50-m spatial resolution there is no heterogeneity, and we can see that the retrieved optical properties and the cost function are nearly zero for every channel combination showing that under the 1-D independent pixel approximation assumption the algorithm uncertainty is negligible. However, we have to acknowledge that this may not be true because we have a unique ice crystal through the whole cloud. The coupling of several spectral regions, such as NIR/SWIR + TIR, which have sensitivities to different parts of the cloud (e.g., vertical heterogeneity), can further complicate the retrieval (Chang et al., 2017). Indeed, in the situation of vertically heterogeneous CER distribution, one would expect that NIR/SWIR or TIR channels

may give different, but physically consistent, CER retrievals when used independently (Kahn et al., 2015; Zhang et al., 2010).

Over 500 m, the addition of the NIR-SWIR information to the TIR channels leads to a decrease of the bias but the cost function strongly increases toward coarser resolution. This indicates that, in these conditions, the aforementioned heterogeneity effects impact the TIR and the NIR/SWIR channels differently. Subsequently, the retrieval algorithm based on a 1-D forward model cannot find a solution that simultaneously reproduces the observed measurements across the entire spectrum. The divergence of heterogeneity impacts across the wavelength spectrum additionally appears to depend on the solar angle. This wavelength dependency is of particular interest as it highlights the importance of properly accounting for subpixel heterogeneity effects when synergistically using multispectral measurements.

3.2. Heterogeneity and 3-D Effects

In this section, horizontal heterogeneity and 3-D radiative effects on the COT (ΔCOT) and effective radius (ΔCER) retrievals are considered. These two quantities are estimated using 3-D RT and the following steps:

1. High spatial resolution (50 m) TIR radiances and/or NIR/SWIR reflectances computed using a 3-D RT code are averaged at a given spatial resolution from 100 m to 10 km.
2. Retrieved optical properties are obtained from the averaged 3-D radiances/reflectances using a 1-D retrieval method.
3. True optical properties are estimated from 50-m optical properties (COT only is averaged because **CER** is set equal to 10 **µm** for the entire cloud layer), linearly averaged to a spatial resolution from 50 m to 10 km.
4. True optical properties are subtracted from retrieved optical properties to obtain ΔCOT and ΔCER.

Figure 3 shows $-\Delta COT$ and ΔCER due to cloud horizontal heterogeneity and 3-D effects as a function of the spatial resolution for five solar angles using TIR channels (8.53, 11.01, and 12.03 **µm**) only (blue lines), NIR/SWIR channels (0.86 and 2.13 **µm**) only (red lines), and the combination of the five channels across the three wavelength ranges (black lines). While horizontal cloud heterogeneity impacts COT and CER mostly at the coarsest spatial resolutions, 3-D effects will mostly impact the highest spatial resolutions (Fauchez, Platnick, Meyer et al., 2017; Fauchez et al., 2018). The combination of these two effects leads to a more complex analysis of Figure 3 compared to Figure 2.

First of all, $-\Delta COT$ looks similar to Figure 2 for the TIR and TIR + NIR/SWIR but not for the NIR/SWIR. Indeed, in the TIR region, the PPH bias due to horizontal cloud heterogeneity dominates over 3-D effects (HRT only), the latter becoming significant only for small scales (below ~250 m) and is, on average, almost nil because it either decreases or increases the radiances depending on the optical thickness and on neighboring pixels (Fauchez, Platnick, Meyer et al., 2017). However, in the NIR/SWIR, the absorption is weaker and the scattering larger, increasing the relative effect of HRT (from a pixel to another), but this is a smoothing effect leading to moderate impact. In addition, for oblique sun, 3-D effects such as side illumination and shadowing will appear, affecting the reflectances (Fauchez et al., 2018) and therefore the retrievals. At finer resolutions than 500 m, the largest $-\Delta COT$ is for NIR/SWIR only retrievals. Very small variations (a percent or less) with the solar azimuth angle ϕ_s are observed for $\theta_s = \mathbf{30}^\circ$. However, $-\Delta COT$ is reduced at $\theta_s = \mathbf{60}^\circ$; $\phi_s = 0°$ because side illumination effect mitigates the HRT (Fauchez et al., 2018). At coarser resolutions than 500 m, the largest $-\Delta COT$ is for TIR only retrievals because the errors are dominated mainly by the PPH bias. Note that for this particular cloud realization, for any solar angles and spatial resolutions, the combination of the five channels (TIR + NIR/SWIR) never gives the smallest $-\Delta COT$.

Concerning ΔCER, results are different according to the solar incidence. For an overhead Sun, the TIR retrieval leads to the largest error. Note that for an overhead sun, 3-D effects on solar reflectances are minimized from shadowing and side illumination, and the stronger PPH bias in the TIR dominates the error. The NIR/SWIR error is almost constant with the spatial resolution, and the (TIR + NIR/SWIR) combination leads to the smallest ΔCER. For oblique Sun, illumination and shadowing become more important. It increases the errors for NIR/SWIR and TIR + NIR/SWIR retrievals, especially below 1 km. TIR ΔCER, being independent on the Sun angle and experiencing a weaker HRT, is the smallest at resolutions finer than 1 km (where large 3-D effects occur), but it is still the largest at coarser resolutions due to its large PPH bias. For NIR/SWIR retrievals, in addition to the HRT, the side illumination and shadowing effect increase ΔCER significantly at resolution finer than 1 km, with minor differences over the Sun azimuth angle. For the relatively small optical thickness of cirrus, 3-D
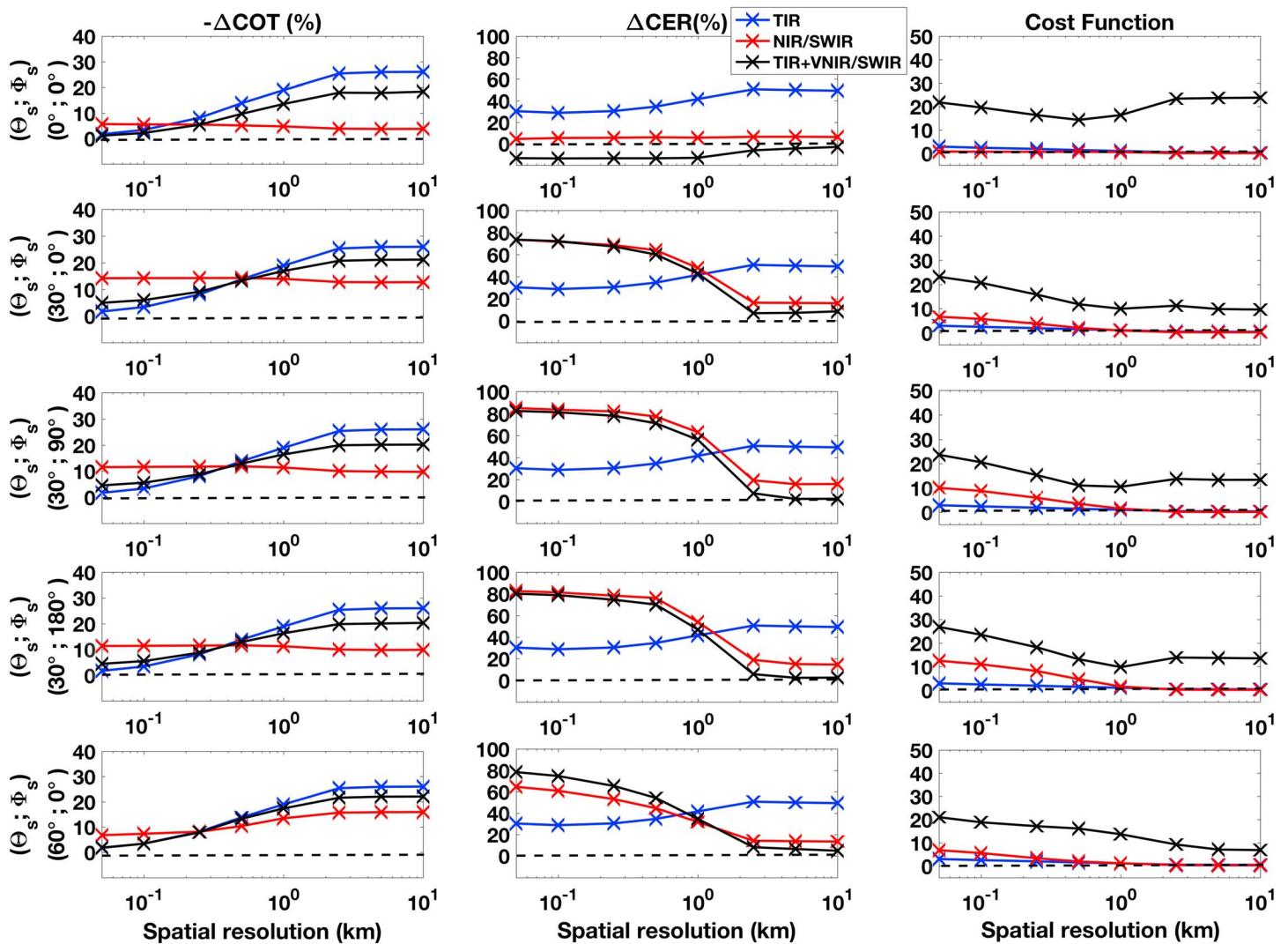
Figure 3. Errors on the (left column) optical thickness and (middle column) effective radius due to cloud horizontal heterogeneity and 3-D effects and the (right column) associated cost function retrieved with an OE in the TIR, NIR/SWIR, and TIR + NIR/SWIR ranges as a function of the spatial resolution and for various solar zenith (θ_s) and azimuth (ϕ_s) angles.

effects act mostly at high spatial resolutions and there is almost no change for resolutions coarser than 1 km by comparison to Figure 2: ΔCER is the largest in the TIR because of the greatest PPH bias. As also seen in Figure 2, the cost function is the largest for the five channel combinations but with different amplitudes than in Figure 2. The local maximums are located for the highest (largest 3-D effects, also seen in the NIR/SWIR) and coarsest (largest PPH bias) spatial resolutions with minimum around 500 m–1 km (except at $\theta_s = 60°$).

As for Figure 2, it is clear from Figure 3 that high 3-D and heterogeneity effects substantially impact the quality of the retrievals. Indeed, the cost function increases for all wavelength configurations where these effects are the highest, which indicates that the retrieval algorithm based on a 1-D RT code has difficulties to find a COT and CER pair that optimally allows a fit to the measurements. It can be noted that in the case of TIR only or NIR/SWIR only, the cost function remains reasonably small, less than 10. However, when merging visible and thermal infrared, this effect becomes significant as HRT and 3-D effects are not the same according to the spectral range used. Also, it is important to mention that beyond 2.5-km spatial resolution, the NIR/SWIR channel retrieval method retrieved the true CER with only few percent error and with a cost function of the of few percent. The CER retrieval using TIR + NIR/SWIR is even closer to the truth while the cost function is high (10 to 30 depending on solar angles).

Table 1

Nonexhaustive List of Satellite Imagers With Their Spatial Resolution and the Estimation of the Retrieval Errors −ΔCOT (Blue Values) and ΔCER (Red Values), Averaged to 10 km, Due to Cirrus Horizontal Heterogeneity and 3-D Effects in the TIR and NIR/SWIR According to Our Study for ASTER (Advanced Spaceborne Thermal Emission and Reflection Radiometer), Landsat-8, MSI (Multispectral Imager), MODIS (Moderate Resolution Imager Spectroradiometer), VIIRS (Visible Infrared Imaging Radiometer Suite), IIR (Imaging Infrared Radiometer), AVHRR-3 (Advanced Very High Resolution Radiometer), 3MI (Multiviewing, Multichannel, Multipolarization Imager), and AIRS (Atmospheric Infrared Sounder)-like Spatial Resolutions but Considering MODIS-like Spectral Characteristics

Instrument	TIR spatial resolution (km)	TIR −ΔCOT (%) ΔCER (%)	NIR/SWIR spatial resolution (km)	NIR/SWIR −ΔCOT (%) ΔCER (%)
ASTER	0.09	4 29	0.015	6-(≥14) 4-(≥82)
Landsat-8	0.1	4 29	0.03	6-(≥14) 4-(≥82)
MSI (EarthCARE)	0.5	13 35	0.5	5–15 6–80
MODIS	1	20 40	0.25	5–15 6–85
			0.5	5–15 6–80
			1	5–12 6–63
VIIRS	0.75(1)	20 40	0.375(0.5)	5–15 6–80
IIR	1	20 40	ø	Ø
AVHRR/3	1	20 40	0.5	5–15 6–80
3MI (Metop-SG)	ø	Ø	4	4–16 6–16
AIRS	13.5	≥30 ≥50	~2	4–16 6–19

Notes. Instrument in light gray is not launched yet. The range of values separated by a hyphen shows the smallest and largest errors depending on the solar angle.

4. Discussions

Fauchez, Platnick, Meyer et al. (2017) have shown that the spatial resolution at which the combination of the PPHB and HRT effects has the smallest impact on TOA TIR radiances is between 100 and 250 m. Below this range the HRT dominates, while the PPH bias dominates above this range. This has also been observed in the CER retrieval from TIR measurements for which the minimum is at 100 m. In the NIR/SWIR, 3-D effects are stronger than in the TIR and include additional effects related to the solar incidence angle such as illumination and shadowing effects. Fauchez et al. (2018) have determined that for ice cloud scenes, the spatial resolution up to which the 3-D effects dominate is about 2.5 km, which is 1 order of magnitude coarser than in the TIR. Because of the relatively small optical thickness of cirrus clouds, the PPH bias is moderate compared to strato-cumulus clouds, even at coarse spatial resolutions, leading to a smaller TOA impact on the reflectance.

From our simulations, we have found that at 1-km spatial resolution, the impact of cloud horizontal hetero-geneity and 3-D effects in the TIR on COT retrievals is about 20% and on CER retrievals is about 40%. From MODIS TIR measurements, Wang, Platnick, Zhang, Meyer, Wing et al. (2016) found typical ice cloud optical property retrieval uncertainties (accounting for measurement, fast RT model, atmospheric profile, and ice crystal habit errors) to be between 5 and 15% for COT and between 20 and 35% for CER. Concerning NIR/SWIR retrievals, we have found a COT error due to cloud horizontal heterogeneity and 3-D effects of 5% to 12%, and between 6% to 63% for CER, depending on solar angle. For the MODIS operational product (Platnick et al., 2017), estimated retrieval uncertainties for a similar cirrus COT and CER, including scene-dependent L1B uncertainties, cloud model, and surface albedo error sources (cloud effective variance, ocean surface wind speed, and direction), are about ~10% for COT and ~20% for 2.1-μm CER retrievals. Like for the TIR retrieval, the errors due to cloud horizontal heterogeneity and 3-D effects are equal to or larger than those

estimated by Wang, Platnick, Zhang, Meyer, Wing et al. (2016) and Platnick et al. (2017). Therefore, those effects are significant and strategies should be developed in order to evaluate them in the retrieved products. Cloud horizontal heterogeneity can be estimated by using higher spatial resolution measurements from a collocated instrument such as the Advanced Spaceborne Thermal Emission and Reflection Radiometer (ASTER) collocated with MODIS on Terra satellite. However, ASTER does not continuously collect data and only observes a small portion of MODIS field of view. 3-D effects are more complicated to address because they require 3-D retrieval algorithms that need the full knowledge of the 3-D radiation field from multiangular measurements (Fauchez, Davis et al., 2017) and are computationally very expensive. Therefore, optimizing an instrument's spatial resolution to mitigate the horizontal heterogeneity effect should be prioritized.

In Table 1, we present the impacts of cloud horizontal heterogeneity and 3-D radiative effects, averaged over the 10-km cirrus field, on COT and CER TIR and NIR/SWIR retrievals from nine space imagers at various spatial resolutions. Note that we made the approximation that all of these instruments have the same spectral characteristics as the MODIS channels used in this study. Therefore, each instrument presented in the table is only here to represent a particular spatial resolution but with MODIS-like spectral characteristics. On the one hand, it seems clear that imagers with very high spatial resolution such as ASTER and Landsat-8 are impacted more in case of NIR/SWIR retrievals. Indeed, 3-D radiative effects, in particular for NIR/SWIR wavelengths, are very strong at these spatial resolutions on the order of tens of meters, resulting in radiation from dozens or hundreds of neighboring pixels modifying the radiances/reflectances of the observed pixels leading to retrieval errors beyond 15% for COT and 80% for CER. Therefore, the benefits of increasing the spatial resolution of space-borne radiometers to better resolve (cirrus) cloud structure, optical property, and variability are highly degraded by 3-D radiative effects. However, for TIR radiance-based cloud retrievals, ASTER and Landsat-8 performed slightly better than the other instruments because in the TIR, the PPHB largely dominates the 3-D effects and at such high-resolution PPHB is drastically reduced. On the other hand, space-borne radiometers with a coarse spatial resolution like AIRS TIR measurements (13.5 km) are not impacted by 3-D radiative effects, but they poorly resolve cloud variability and are therefore highly impacted by the PPH bias. The best spatial resolution range appears to be in the 1–2 km such as for MODIS in the NIR/SWIR ($-\Delta$COT: 5%–12% and ΔCER: 6%–63%). Note that this spatial resolution range has also been found by Davis et al. (1997) for stratocumulus clouds.

5. Conclusions

In this paper, we investigated the impact of cirrus cloud heterogeneities and 3-D RT effects on the COT and ice CER retrieved with NIR/SWIR, TIR, or NIR/SWIR and TIR information, for spatial resolutions ranging from 50 m to 10 km. In this study, we use only one 3DCLOUD cirrus field generated with "realistic in the average sense" values of macroscale and optical properties such as the visible optical depth (close to 1), the geometrical thickness (close to 2 km), the spectral slope of the optical thickness (close to $-5/3$), and the inhomogeneous parameter (close to 1.0). This cirrus field can thus be considered as quite representative of a large variety of cirrus clouds. Nevertheless, further theoretical studies, with different kinds of cirrus cloud structures and more variety of the macroscale and optical properties, together with different dynamic conditions (vertical wind shear for example), are needed to completely quantify effects of cirrus inhomogeneity on their radiative properties.

The RT was performed with the 3DMCPOL code in 3-D and 1-D RT configurations at various spatial resolutions for three TIR wavelengths (8.53, 11.01, and 12.03 μm), one in the NIR (0.86 μm), and one in the SWIR (2.13 μm). The cloud properties have been retrieved with the ML OE code (Sourdeval et al., 2015) using either the three TIR channels only, the NIR and SWIR channels only, or a combination of all five channels. Large differences of tens of percent have been observed between the three retrievals. When considering only horizontal heterogeneity effects $-\Delta$COT is the smallest for NIR/SWIR (few percent) because the PPH bias is smaller than for TIR. ΔCER is smallest for NIR/SWIR and TIR + NIR/SWIR five channel retrievals (0 to few percent). Under 500 m, sub-pixel heterogeneity effects are negligible, and the situation is equivalent to retrieving a 1-D homogeneous field. Retrievals using a wide range of channels have demonstrated smaller biases. However, above 500 m, the strong increase of the cost function suggests large differences of PPH bias between the TIR and SWIR/NIR channels and therefore large incertitude in the retrieval (the cost function going up to ~40).

It is important to note that simulations were run using a fixed ice crystal size and shape and cloud altitude, while the amplitude of the retrieval errors may change as a function of the cirrus altitude, geometrical thickness, and CER vertical distribution, mostly due to the sensitivity of TIR channels to those parameters. From

Fauchez et al. (2015), we know that higher cloud top altitudes will increase the retrieval error because of the larger BT contrast between the cloud top and the surface. Larger geometrical thickness will reduce the retrieval error because the emission temperature of the bottom of the cloud will be closer to that of the surface. Concerning the CER, cloud absorption in the TIR decreases when increasing CER from 5 to 20 μm (above TIR retrieval is less sensitive), while it stays fairly constant at 0.86 μm but increases at 2.13 μm. Therefore, for larger CER, the PPHB is expected to be smaller for TIR retrieval and larger for NIR/SWIR retrieval. This could consequently lead to a better agreement between TIR and NIR/SWIR retrievals. Also, because cloud-top NIR/SWIR or TIR observations have different sensitivities to distinct parts of the cloud, it would be expected that the channels may give different, but physically consistent, CER retrievals when used independently. Combined together, a unique CER retrieval may be found but with an associated increase of the solution cost function. The impact of the vertical heterogeneity, while warranting investigation, is out of the scope of this paper.

When 3-D effects (horizontal radiative transport and side illumination and shadowing effects for oblique Sun) are added to the horizontal heterogeneity effect, TIR retrievals provide the smallest −ΔCOT and ΔCER below 1 km because of weak horizontal radiative transport and no 3-D effects but the largest −ΔCOT and ΔCER at resolutions coarser than 1 km. NIR/SWIR retrievals lead to the largest −ΔCOT at the highest spatial resolutions (below 250 m) because of 3-D effects, but the smallest −ΔCOT for resolutions coarser than 500 m because of a weaker PPH bias than in TIR. The only configuration where TIR + NIR/SWIR retrieval is smaller than TIR or NIR/SWIR only is for ΔCER retrieval above 2.5-km spatial resolution. Therefore, the use of multiple channels across various wavelength ranges does not always improve the retrieval by comparison to either TIR or NIR/SWIR retrievals because the spectral dependence of heterogeneity and 3-D effects significantly impacts the retrievals. Indeed, the cost function, which quantifies the radiative coherence of the retrievals with the observations, sharply increases when merging visible and thermal infrared measurements. This has important implications as retrieval methods now tend to merge information from different wavelengths in order to constrain cloud retrievals without accounting or correcting for 3-D radiative effects. Also, future satellite missions will carry spectrometers with high spatial resolution (e.g., EarthCare and Metop-SG), more sensitive to the latter effects. Synergistic multispectral retrievals of cloud properties have recently become common practice, as merging information from multiple wavelengths often allows for better constrained retrievals as well as a wider sensitivity to different cloud types. However, this study suggests that caution should be taken when synergistically using various spectral ranges from high resolution instruments, for example, by adding uncertainties representative of different 3-D radiative effects and PPH bias. Therefore, a compromise has to be found to mitigate 3-D radiative effects and PPH bias without sacrificing the information content available for the retrieval. Further investigation nevertheless remains necessary to evaluate the generality of this conclusion.

Code Availability

The simulated data used in this study were generated by the 3DCLOUD (Szczap et al., 2014) and 3DMCPOL (Cornet et al., 2010; Fauchez et al., 2014) closed-source codes.

Please contact the authors for more information.

References

Ahlgrimm, M., & Forbes, R. M. (2016). *Regime dependence of cloud condensate variability observed at the* `Atmospheric Radiation Measurement` *sites: Regime dependence of cloud condensate variability* (Vol. 142, pp. 1605–1617). United Kingdom: Web. https://doi.org/10.1002/qj.2783

Ahlgrimm, M., & Forbes, R. M. (2017). *Regime dependence of ice cloud heterogeneity—A convective life-cycle effect?: Ice cloud heterogeneity* (Vol. 143, pp. 3259–3268). United Kingdom: Web. https://doi.org/10.1002/qj.3178

Alkasem, A., Szczap, F., Cornet, C., Shcherbakov, V., Gour, Y., Jourdan, O., et al. (2017). Effects of cirrus heterogeneity on lidar CALIOP/CALIPSO data. *Journal of Quantitative Spectroscopy & Radiative Transfer*, *202*, 38–49. https://doi.org/10.1016/j.jqsrt.2017.07.005

American Meteorological Society (2012)."Cirrus." Glossary of meteorology. [Available online at http://glossary.ametsoc.org/wiki/Cirrus.]

Baran, A. J. (2009). A review of the light scattering properties of cirrus. *Journal of Quantitative Spectroscopy & Radiative Transfer*, *110*(14-16), 1239–1260. https://doi.org/10.1016/j.jqsrt.2009.02.026

Boucher, O., Randall, D., Artaxo, P., Bretherton, C., Feingold, G., Forster, P., et al. (2013). *The physical science basis. Contribution of working group I to the fifth assessment report of the Intergovernmental Panel on Climate Change*, book section 7 (pp. 571–658). Cambridge, United Kingdom and New York, NY, USA: Cambridge University Press.

Cahalan, R. F., Ridgway, W., Wiscombe, W. J., Bell, T. L., & Snider, J. B. (1994). The albedo of fractal stratocumulus clouds. *Journal of the Atmospheric Sciences*, *51*(16), 2434–2455. https://doi.org/10.1175/1520-0469(1994)051<2434:TAOFSC>2.0.CO;2

Chang, K.-W., L'Ecuyer, T. S., Kahn, B. H., & Natraj, V. (2017). Information content of visible and midinfrared radiances for retrieving tropical ice cloud properties. *Journal of Geophysical Research: Atmospheres*, *122*, 4944–4966. https://doi.org/10.1002/2016JD026357

Cooper, S. J., & Garrett, T. J. (2010). Identification of small ice cloud particles using passive radiometric observations. *Journal of Applied Meteorology and Climatology*, *39*, 2334–2347.

Cooper, S. J., L'Ecuyer, T. S., Gabriel, P., Baran, A. J., & Stephens, G. L. (2007). Performance assessment of a five-channel estimation-based ice cloud retrieval scheme for use over the global oceans. *Journal of Geophysical Research*, *112*, D04207. https://doi.org/10.1029/2006JD007122

Cornet, C., C-Labonnote, L., & Szczap, F. (2010). Three-dimensional polarized Monte Carlo atmospheric radiative transfer model (3DMCPOL): 3-D effects on polarized visible reflectances of a cirrus cloud. *Journal of Quantitative Spectroscopy & Radiative Transfer*, *111*(1), 174–186. https://doi.org/10.1016/j.jqsrt.2009.06.013

Davis, A., Marshak, A., Cahalan, R., & Wiscombe, W. (1997). The Land-sat scale break in stratocumulus as a three-dimensional radiative transfer effect: Implications for cloud remote sensing. *Journal of the Atmospheric Sciences*, *54*(2), 241–260. https://doi.org/10.1175/1520-0469(1997)054<0241:TLSBIS>2.0.CO;2

Dubuisson, P., Giraud, V., Pelon, J., Cadet, B., & Yang, P. (2008). Sensitivity of thermal infrared radiation at the top of the atmosphere and the surface to ice cloud microphysics. *Journal of Applied Meteorology and Climatology*, *47*(10), 2545–2560. https://doi.org/10.1175/2008JAMC1805.1

Fauchez, T., Cornet, C., Szczap, F., & Dubuisson, P. (2012). *Assessment of cloud heterogeneities effects on brightness temperatures simulated with a 3-D Monte-Carlo code in the thermal infrared*, (p. 4). Berlin, Germany: International Radiation Symposium proceeding.

Fauchez, T., Cornet, C., Szczap, F., Dubuisson, P., & Rosambert, T. (2014). Impacts of cirrus clouds heterogeneities on TOA thermal infrared radiation. *Atmospheric Chemistry and Physics*, *14*(11), 5599–5615. https://doi.org/10.5194/acp-14-5599-2014

Fauchez, T., Davis, A. B., Cornet, C., Szczap, F., Platnick, S., Dubuisson, P., & Thieuleux, F. (2017). A fast hybrid (3-D/1-D) model for thermal radiative transfer in cirrus via successive orders of scattering. *Journal of Geophysical Research: Atmospheres*, *122*, 344–366. https://doi.org/10.1002/2016JD025607

Fauchez, T., Dubuisson, P., Cornet, C., Szczap, F., Garnier, A., Pelon, J., & Meyer, K. (2015). Impacts of cloud heterogeneities on cirrus optical properties retrieved from space-based thermal infrared radiometry. *Atmospheric Measurement Techniques*, *8*(2), 633–647. https://doi.org/10.5194/amt-8-633-2015

Fauchez, T., Platnick, S., Meyer, K., Cornet, C., Szczap, F., & Várnai, T. (2017). Scale dependence of cirrus horizontal heterogeneity effects on TOA measurements—Part I: MODIS brightness temperatures in the thermal infrared. *Atmospheric Chemistry and Physics*, *17*(13), 8489–8508. https://doi.org/10.5194/acp-17-8489-2017

Fauchez, T., Platnick, S., Sourdeval, O., Meyer, K., Cornet, C., Zhang, Z., & Szczap, F. (2017). Cirrus heterogeneity effects on cloud optical properties retrieved with an optimal estimation method from MODIS VIS to TIR channels. *AIP Conference Proceedings*, *1810*(1), 040002.

Fauchez, T., Platnick, S., Várnai, T., Meyer, K., Cornet, C., & Szczap, F. (2018). Scale dependence of cirrus heterogeneity effects. Part II: MODIS NIR and SWIR channels. *Atmospheric Chemistry and Physics*, *18*, 12,105–12,121. https://doi.org/10.5194/acp-18-12105-2018

Fusina, F., Spichtinger, P., & Lohmann, U. (2007). Impact of ice supersaturated regions and thin cirrus on radiation in the midlatitudes. *Journal of Geophysical Research*, *112*, D24S14. https://doi.org/10.1029/2007JD008449

Garnier, A., Pelon, J., Dubuisson, P., Faivre, M., Chomette, O., Pascal, N., & Kratz, D. P. (2012). Retrieval of cloud properties using CALIPSO `Imaging Infrared Radiometer`. Part I: Effective emissivity and optical depth. *Journal of Applied Meteorology and Climatology*, *51*(7), 1407–1425. https://doi.org/10.1175/JAMC-D-11-0220.1

Garnier, A., Pelon, J., Dubuisson, P., Yang, P., Faivre, M., Chomette, O., et al. (2013). Retrieval of cloud properties using CALIPSO `Imaging Infrared Radiometer`. Part II: Effective diameter and ice water path. *Journal of Applied Meteorology and Climatology*, *52*(11), 2582–2599. https://doi.org/10.1175/JAMC-D-12-0328.1

Heidinger, A. K., Foster, M. J., Walther, A., & Zhao, X. (2014). The pathfinder atmospheres-extended AVHRR climate dataset. *Bulletin of the American Meteorological Society*, *95*(6), 909–922. https://doi.org/10.1175/BAMS-D-12-00246.1

Heymsfield, A. J., Krämer, M., Luebke, A., Brown, P., Cziczo, D. J., Franklin, C., et al. (2017). Cirrus clouds. *Meteorological Monographs*, *58*, 2.1–2.26. https://doi.org/10.1175/AMSMONOGRAPHS-D-16-0010.1

Hill, P. G., Hogan, R. J., Manners, J., & Petch, J. C. (2012). Parametrizing the horizontal inhomogeneity of ice water content using CloudSat data products. *Quarterly Journal of the Royal Meteorological Society*, *138*(668), 1784–1793. https://doi.org/10.1002/qj.1893

Hill, P. G., Morcrette, C. J., & Boutle, I. A. (2015). A regime-dependent parametrization of subgrid-scale cloud water content variability. *Quarterly Journal of the Royal Meteorological Society*, *141*(691), 1975–1986. https://doi.org/10.1002/qj.2506

Hogan, R. J., & Kew, S. F. (2005). A 3D stochastic cloud model for investigating the radiative properties of inhomogeneous cirrus clouds. *Quarterly Journal of the Royal Meteorological Society*, *131*(611), 2585–2608. https://doi.org/10.1256/qj.04.144

Inoue, T. (1985). On the temperature and effective emissivity determination of semi-transparent cirrus clouds by bi-spectral measurements in the 10 μm window region. *Journal of the Meteorological Society of Japan*, *63*(1), 88–99. https://doi.org/10.2151/jmsj1965.63.1_88

Kahn, B. H., Irion, F. W., Dang, V. T., Manning, E. M., Nasiri, S. L., Naud, C. M., et al. (2014). The Atmospheric Infrared Sounder version 6 cloud products. *Atmospheric Chemistry and Physics*, *14*, 399–426. https://doi.org/10.5194/acp-14-399-2014

Kahn, B. H., Schreier, M. M., Yue, Q., Fetzer, E. J., Irion, F. W., Platnick, S., et al. (2015). Pixel-scale assessment and uncertainty analysis of AIRS and MODIS ice cloud optical thickness and effective radius. *Journal of Geophysical Research: Atmospheres*, *120*, 11,669–11,689. https://doi.org/10.1002/2015JD023950

Kato, S., & Marshak, A. (2009). Solar zenith and viewing geometry-dependent errors in satellite retrieved cloud optical thickness: Marine stratocumulus case. *Journal of Geophysical Research*, *114*, D01202. https://doi.org/10.1029/2008JD010579

Kuo, K. S., Welch, R. M. R., & Szngupta, K. (1988). Structural and textural characteristics of cirrus clouds observed using high spatial resolution LANDSAT imagery. *Journal of Applied Meteorology*, *27*(11), 1242–1260. https://doi.org/10.1175/1520-0450(1988)027<1242:SATCOC>2.0.CO;2

Lynch, D., Sassen, K., Starr, D. O., &Stephens, G. L. (2002).Cirrus, Oxford University Press

Marks, C. J., & Rodgers, C. D. (1993). A retrieval method for atmospheric composition from limb emission measurements. *Journal of Geophysical Research*, *98*, 14939–14953.

Matus, A. V., & L'Ecuyer, T. S. (2017). The role of cloud phase in Earth's radiation budget. *Journal of Geophysical Research: Atmospheres*, *122*, 2559–2578. https://doi.org/10.1002/2016JD025951

Minnis, P., Sun-Mack, S., Young, D., Heck, P., Garber, D., Chen, Y., et al. (2011). *CERES edition-2 cloud property retrievals using TRMM VIRS and Terra and Aqua MODIS data x2014; part I: Algorithms. IEEE Transactions onGeoscience and Remote Sensing*, *49*(11), 4374–4400. https://doi.org/10.1109/TGRS.2011.2144601

Oreopoulos, L., Cho, N., & Lee, D. (2017). New insights about cloud vertical structure from CloudSat and CALIPSO observations. *Journal of Geophysical Research: Atmospheres*, *122*, 9280–9300. https://doi.org/10.1002/2017JD026629

Parol, F., Buriez, J. C., Brogniez, G., & Fouquart, Y. (1991). Information content of AVHRR channels 4 and 5 with respect to the effective radius of cirrus cloud particles. *Journal of Applied Meteorology*, *30*(7), 973–984. https://doi.org/10.1175/1520-0450-30.7.973

Platnick, S., Meyer, K. G., King, M. D., Wind, G., Amarasinghe, N., Marchant, B., et al. (2017). The MODIS cloud optical and microphysical products: Collection 6 updates and examples from Terra and Aqua. *IEEE Transactions on Geoscience and Remote Sensing*, *PP*(99), 1–24.

Pujol, O. (2015). Comment on the (misused) concept of photon in radiative transfer, and proposition of a neologism. *Journal of Quantitative Spectroscopy and Radiative Transfer*, *159*, 29–31. https://doi.org/10.1016/j.jqsrt.2015.02.024

Rodgers, C. D. (2000). *Inverse methods for atmospheric sounding theory and practice*. World Scientific. https://doi.org/10.1142/3171

Sanderson, B., Piani, C., Ingram, W. J., Stone, D. A., & Allen, M. R. (2008). Towards constraining climate sensitivity by linear analysis of feedback patterns in thousands of perturbed-physics GCM simulations. *Climate Dynamics*, *30*(2-3), 175–190. https://doi.org/10.1007/s00382-007-0280-7

Shonk, J. K. P., Hogan, R. J., Edwards, J. M., & Mace, G. G. (2010). Effect of improving representation of horizontal and vertical cloud structure on the Earth's global radiation budget. Part I: Review and parametrization. *Quarterly Journal of the Royal Meteorological Society*, *136*(650), 1191–1204. https://doi.org/10.1002/qj.647

Sourdeval, O., Labonnote, L. C., Baran, A. J., & Brogniez, G. (2015). A methodology for simultaneous retrieval of ice and liquid water cloud properties. Part I: Information content and case study. *Quaterly Journal of the Royal Meteorological Society*, *141*(688), 870–882. https://doi.org/10.1002/qj.2405

Sourdeval, O., Labonnote, L. C., Baran, A. J., Mulmenstadt, J., & Brogniez, G. (2016). A methodology for simultaneous retrieval of ice and liquid water cloud properties. Part II: Near-global retrievals and evaluation against A-train products. *Quaterly Journal of the Royal Meteorological Society*, *142*(701), 3063–3081. https://doi.org/10.1002/qj.2889

Sourdeval, O., Brogniez, G., Pelon, J., Labonnote, L. C., Dubuisson, P., Parol, F., et al. (2012). Validation of IIR/CALIPSO level 1 measurements by comparison with collocated airborne observations during CIRCLE-2 and Biscay'08 campaigns. *Journal of Atmospheric and Oceanic Techology*, *29*(5), 653–667. https://doi.org/10.1175/JTECH-D-11-01143.1

Stephens, G. L., Gabriel, P. M., & Tsay, S.-C. (1991). Statistical radiative transport in one-dimensional media and its application to the terrestrial atmosphere. *Transport Theory and Statistical Physics*, *20*(2-3), 139–175. https://doi.org/10.1080/00411459108203900

Szczap, F., Gour, Y., Fauchez, T., Cornet, C., Faure, T., Jourdan, O., & Dubuisson, P. (2014). 3DCloud, a fast and flexible 3D cloud optical depth generator based on drastically simplified basic atmospheric equations and Fourier transform framework. Applications to stratocumulus, cumulus and cirrus cloud fields. *Geoscientific Model Development*, *7*, 1779–1801.

Szczap, F., Isaka, H., Saute, M., Guillemet, B., & Gour, Y. (2000). Inhomogeneity effects of 1D and 2D bounded cascade model clouds on their effective radiative properties. *Physics and Chemistry of the Earth, Hydrology, Oceans and atmosphere*, *25*(2), 83–89. https://doi.org/10.1016/S1464-1909(99)00129-X

Varnai, T., & Marshak, A. (2001). Statistical analysis of the uncertainties in cloud optical depth retrievals caused by three-dimensional radiative effects. *Journal of the Atmospheric Sciences*, *58*(12), 1540–1548. https://doi.org/10.1175/1520-0469(2001)058<1540:SAOTUI>2.0.CO;2

Wang, C., Platnick, S., Zhang, Z., Meyer, K., Wing, G., & Yang, P. (2016). Retrieval of ice cloud optical properties using an optimal estimation algorithm and MODIS infrared observations: Part II: Retrieval evaluation. *Journal of Geophysical Research*, *121*(10), 5827–5845.

Wang, C., Platnick, S., Zhang, Z., Meyer, K., & Yang, P. (2016). Retrieval of ice cloud optical properties using an optimal estimation algorithm and MODIS infrared observations: Part I: Forward model, error analysis, and information content. *Journal of Geophysical Research*, *121*(10), 5809–5826.

Xiong, X., Angal, A., Barnes, W., Chen, H., Chaing, V., Geng, X., et al. (2017). A updates of MODIS on-orbit calibration uncertainty assessments. *Proceedings of SPIE? Sensors, Systems XXII*, *10,402*, 104020M.

Xiong, X., Sun, J., Wu, A., Chiang, K.-F., Esposito, J., & Barnes, W. (2005). Terra and Aqua MODIS calibration algorithms and uncertainty analysis. *Proceedings of SPIE: Sensors, Systems, and Next Generation of Satellites IX*, *5978*, 59780V.

Yang, P., Bi, L., Baum, B., Liou, K.-N., Kattawar, G., Mishchenko, M., & Cole, B. (2013). Spectrally consistent scattering, absorption, and polarization properties of atmospheric ice crystals at wavelengths from 0.2 to 100 μm. *Journal of the Atmospheric Sciences*, *70*(1), 330–347. https://doi.org/10.1175/JAS-D-12-039.1

Zhang, Y., Macke, A., & Albers, F. (1999). Effect of crystal size spectrum and crystal shape on stratiform cirrus radiative forcing. *Atmospheric Research*, *52*(1-2), 59–75. https://doi.org/10.1016/S0169-8095(99)00026-5

Zhang, Z., Ackerman, A. S., Feingold, G., Platnick, S., Pincus, R., & Xue, H. (2012). Effects of cloud horizontal heterogeneity and drizzle on remote sensing of cloud droplet effective radius: Case studies based on large-eddy simulations. *Journal of Geophysical Research*, *117*, D19208. https://doi.org/10.1029/2012JD017655

Zhang, Z., & Platnick, S. (2011). An assessment of differences between cloud effective particle radius retrievals for marine water clouds from three MODIS spectral bands. *Journal of Geophysical Research*, *116*, D20215. https://doi.org/10.1029/2011JD016216

Zhang, Z., Platnick, S., Yang, P., Heidinger, A. K., & Comstock, J. M. (2010). Effects of ice particle size vertical inhomogeneity on the passive remote sensing of ice clouds. *Journal of Geophysical Research*, *115*, D17203. https://doi.org/10.1029/2010JD013835

Zhang, Z., Werner, F., Cho, H. M., Wind, G., Platnick, S., Ackerman, A. S., et al. (2016). A framework based on 2-D Taylor expansion for quantifying the impacts of sub-pixel reflectance variance and covariance on cloud optical thickness and effective radius retrievals based on the bi-spectral method. *Journal of Geophysical Research: Atmospheres*, *121*, 7007–7025. https://doi.org/10.1002/2016JD024837

Zhou, Y., Sun, X., Zhang, R., Zhang, C., Li, H., Zhou, J., & Li, S. (2017). Influences of cloud heterogeneity on cirrus optical properties retrieved from the visible and near-infrared channels of MODIS/SEVIRI for flat and optically thick cirrus clouds. *Journal of Quantitative Spectroscopy & Radiative Transfer*, *187*, 232–246. https://doi.org/10.1016/j.jqsrt.2016.09.020

Zinner, T., & Mayer, B. (2006). Remote sensing of stratocumulus clouds: Uncertainties and biases due to heterogeneity. *Journal of Geophysical Research*, *111*, D14209. https://doi.org/10.1029/2005JD006955

Zinner, T., Wind, G., Platnick, S., & Ackerman, A. S. (2010). Testing remote sensing on artificial observations: Impact of drizzle and 3-D cloud structure on effective radius retrievals. *Atmospheric Chemistry and Physics*, *10*(19), 9535–9549. https://doi.org/10.5194/acp-10-9535-2010